CHEMICAL PHYSICS

Polyelectrolytes induce water-water correlations that result in dramatic viscosity changes and nuclear quantum effects

J. Dedic, H. I. Okur, S. Roke*

Ions interact with water via short-ranged ion-dipole interactions. Recently, an additional unexpected long-ranged interaction was found: The total electric field of ions influences water-water correlations over tens of hydration shells, leading to the Jones Ray effect, a 0.3% surface tension depression. Here, we report such long-range interactions contributing substantially to both molecular and macroscopic properties. Femtosecond elastic second harmonic scattering (fs-ESHS) shows that long-range electrostatic interactions are remarkably strong in aqueous polyelectrolyte solutions, leading to an increase in water-water correlations. This increase plays a role in the reduced viscosity, which changes more than two orders of magnitude with polyelectrolyte concentration. Using D_2O instead of H_2O shifts both the fs-ESHS and the viscosity curve by a factor of ~10 and reduces the maximum viscosity value by 20 to 300%, depending on the polyelectrolyte. These phenomena cannot be explained using a mean-field approximation of the solvent and point to nuclear quantum effects.

INTRODUCTION

Most biochemical reactions occur in aqueous environments, underlining the importance of water for life. More than just a passive background, water actively participates in various processes, such as enzyme and ion channel activity, protein folding and stability, self-assembly (*1*), molecular recognition (*2*, *3*), charging (*4*), and lubrication (*5*). This is possible because water molecules are strongly responsive to electrostatic fields of simple ions, charged macromolecules such as polyelectrolytes, or polar groups. To understand the complex role that water plays in biochemical processes, it is necessary to study the interaction of ions and ionic groups with water on both the molecular and macroscopic levels. It has been found that various macroscopic properties of bulk aqueous solutions are influenced by ions, such as the dynamic viscosity and the surface tension (*6*–*8*). The changes in these properties have their origins within the molecular nature of the interactions between ions and water. The molecular-level interaction of ions with water has been investigated for electrolyte solutions with ionic strengths of >0.1 M using x-ray scattering (*9*), neutron scattering (*10*), infrared spectroscopy (*11*), Raman scattering (*12*, *13*), terahertz spectroscopy (*14*), and molecular dynamics (MD) simulations (*15*–*18*), among others. These studies show that the molecular structure of water in the vicinity of ions is strongly influenced by the valence, polarizability, and size of the ion (*19*–*21*) and that significant perturbations of the structure and dynamics of liquid water are observed within the first three hydration shells. In addition, the ion-water interaction is influenced only minimally by nuclear quantum effects (*22*–*25*).

Recent femtosecond elastic second harmonic scattering (fs-ESHS) experiments performed by us (*24*, *26*) and others (*27*), together with subsequent computational studies (*15*, *28*, *29*), have provided a new dimension to the understanding of water-ion interactions. fs-ESHS experiments are performed by illuminating an aqueous solution with 190 fs laser pulses at 1028 nm and detecting the light scattered at the second harmonic (SH) wavelength (514 nm). Coherently emitted SH light reports on orientational correlations between molecules and is thus sensitive to hydrogen (H)–bonding. Performing fs-ESHS experiments on 21 different aqueous electrolyte solutions spanning a concentration range from 1 μM to 0.1 M revealed a universal increase in the fs-ESHS intensity, but only for polarization combinations that contain coherent emission. This increase was further absent for neutral solutes and displayed remarkably different curves for H_2O and D_2O. It was proposed that the total long-ranged electrostatic field of the ions already present at low salt concentrations perturbs the water-water correlations in the H-bond network of water and is subject to a significant and as of yet unexplained nuclear quantum effect. Revisiting key elements of the experiments and interpretation here, Fig. 1A shows fs-ESHS data for NaCl in H_2O and D_2O solutions adapted from (*24*, *30*). It can be seen that the fs-ESHS response already increases at a salt concentration of 10 μM and saturates at ~1 mM. In an fs-ESHS experiment, the nonlinear optical polarization of a liquid composed of noncentrosymmetric molecules is measured. This polarization arises from two sources (*31*–*33*): The first contribution arises from the polarization of individual molecules and gives rise to incoherent (hyper-Rayleigh) scattering (*31*, *34*). It occurs in all polarization combinations of the in- and outgoing optical fields. The second contribution arises from the coherent addition of SH signal from different but orientationally correlated molecules. This coherent contribution can be measured only in certain polarization combinations of the optical fields, e.g., with all beams polarized parallel to the scattering plane (PPP polarization combination). The response in Fig. 1A therefore arises from water (because the ions used are centrosymmetric) and reports on orientational correlations between different water molecules. Because these correlations are already observed at ion separations of ~20 nm, the phenomenon reports on long-ranged interactions. The D_2O solution in Fig. 1A displays the same trend but with a lower saturation value and higher onset concentration compared to H_2O. Although the H_2O curve in the PPP polarization combination in Fig. 1A can be modeled using a mean-field Debye-Hückel model that describes the influence of the total electrostatic field in the solution on the molecular orientational order (*24*, *26*, *28*, *29*), this model fails to

Laboratory for Fundamental BioPhotonics (LBP), Institute of Bioengineering (IBI), and Institute of Materials Science (IMX), School of Engineering (STI), and Lausanne Centre for Ultrafast Science (LACUS), École Polytechnique Fédérale de Lausanne (EPFL), CH-1015 Lausanne, Switzerland.
*Corresponding author. Email: sylvie.roke@epfl.ch

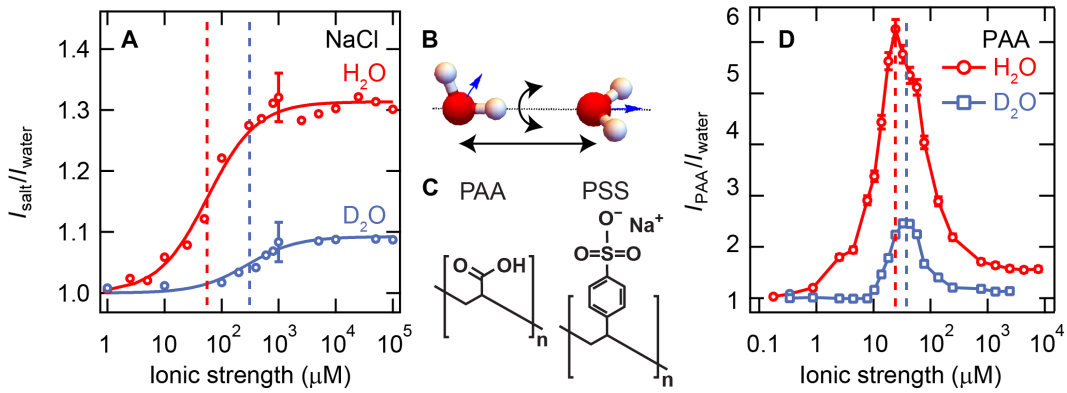

Fig. 1. Long-range distortion of the orientational order of water. (**A**) fs-ESHS intensities, relative to that of pure water, of NaCl in H_2O and D_2O obtained at a scattering angle of 90° in the PPP polarization combination. The fs-ESHS data are adapted from (*24*, *30*). The dashed lines indicate the concentrations of half saturation. (**B**) Illustration of two H-bonded water molecules that are orientationally correlated. The black arrows represent different axes, along which H-bonds can be broken. fs-ESHS is mostly sensitive to the breaking of this H-bond via rotation (black curved arrow). In a D_2O molecule, the H-bond bending mode is predicted to be stronger than in H_2O, while the H-bond stretching mode is expected to be weaker due to nuclear quantum effects. (**C**) Molecular structures of PAA and PSS polyelectrolytes. (**D**) fs-ESHS intensities, relative to that of pure water, of PAA in H_2O and D_2O obtained at a scattering angle of 90°. The dashed blue and red lines indicate peak intensity concentrations. All fs-ESHS data were recorded with beams polarized parallel to the horizontal scattering plane (PPP). The molecular weight of PAA was 450 kDa.

explain the large discrepancy between H_2O and D_2O (as well as other models that represent water only by a dielectric constant). The H_2O/D_2O difference therefore suggests that ions influence collective H-bonding interactions. Water has two distinct modes for breaking H-bonds (illustrated in Fig. 1B), whose relative strengths are different in H_2O and D_2O. Because fs-ESHS probes orientational correlations between water molecules, it has more sensitivity toward detecting H-bond breaking by bending rather than stretching and can distinguish H_2O from D_2O.

The weak ion-induced restructuring of the H-bond network of water was connected to the Jones-Ray effect (*35*), which entails an anomalous and isotope-dependent ~0.3% reduction of the surface tension at the fs-ESHS saturation concentrations. The ion-induced increase in orientational order in the aqueous bulk solution gives rise to an entropic penalty, which causes a reduction in the surface tension (*24*, *35*, *36*). This long-range interaction of the ionic electrostatic field with water is a new and poorly understood phenomenon that warrants further investigation. One could ask how long-ranged and important water ordering can be because, until now, the reported effects it causes represent only a minor (0.3%) change in macroscopic properties (*37*).

Here, we report that long-range reordering of the H-bond structure of water via weakly screened electrostatic interactions in polyelectrolyte solutions causes significant changes of the reduced specific viscosity. Anionic polyelectrolytes, poly(acrylic acid) (PAA), and poly(styrene sulfonate) (PSS) are shown to strongly enhance the orientational order of water, starting at polyelectrolyte concentrations as low as 1 nM and ionic strength of 1 μM. The molecular structures of PAA and PSS are displayed in Fig. 1C. The changes in the orientational order of water are more pronounced in H_2O than in D_2O, consistent with the behavior observed in the solutions of simple salts. The reduced specific viscosity of the polyelectrolyte solutions follows a similar trend as the water ordering, for both H_2O and D_2O, and changes of more than two orders of magnitude are observed. We conclude that long-range interactions between spatially correlated ionic groups on the polyelectrolytes and the H-bond network have a significant impact on the reduced viscosity. Although traditional mean-field models based on inter- and intra-polyelectrolyte correlations can qualitatively explain the viscosity anomaly in H_2O, the models fail to predict the discrepancy between H_2O and D_2O (*38*, *39*). This points to water-water correlations having an influence on the anomalous viscosity of polyelectrolyte solutions. In addition, our data suggest that H-bond breaking through rotations occurs more readily than through H-bond stretching (Fig. 1B) and is relatively more important for viscosity.

RESULTS AND DISCUSSION

Femtosecond snapshots of long-range order

The orientational correlations between water molecules in solutions of PAA and PSS were measured at different concentrations (ionic strengths). The ionic strength (I) of the solution, due to the dissolved and partially dissociated polyelectrolytes, was calculated as $I = 0.5 c_m f$, where c_m is the monomer concentration in M and f is the percentage of dissociated counterions. According to Manning's theory of counterion condensation (*40*, *41*), the degree of ionization is $f = b/\lambda_B = 0.35$, where b = 0.25 nm is the distance between ionizable groups on the polyelectrolyte chain and $\lambda_B = e^2/4\pi\varepsilon_0\varepsilon k_B T = 0.71$ nm is the Bjerrum length in water, with e the elementary charge, ε_0 the vacuum permittivity, $\varepsilon = 78.5$ the dielectric constant of water, k_B the Boltzmann constant, and temperature $T = 298$ K. Figure 1D shows the fs-ESHS response of PAA solutions of different ionic strength recorded at a scattering angle $\theta = 90°$, with all beams polarized in the horizontal scattering plane. The intensities are normalized with respect to the fs-ESHS intensity of the pure solvent, and data for both H_2O and D_2O solutions are shown. It can be seen that the fs-ESHS response from H_2O solutions increases from a value of 1 at near-infinite dilution and reaches a maximum of 6.2, after which the intensity drops again and levels off above an ionic strength of ~1 mM. The increase in the scattered intensity with concentration might be intuitively interpreted in terms of increasing the number density of bare polyelectrolytes. This simple explanation is, however, contradicted by the subsequent decrease in fs-ESHS intensity. Moreover, incoherent fs-ESHS measurements [recorded with all beams polarized in the direction vertical to

the scattering plane (SSS)] of the same solutions, shown in fig. S1, display no increase in the fs-ESHS response at the concentrations used here. If the bare polyelectrolytes contributed significantly to the SH signal, we would expect to see an increase in the incoherent response in fig. S1. The reason why the contribution of the bare polyelectrolytes is insignificant compared to their hydration shells can be understood by noting that in a nonresonant fs-ESHS experiment, the emitted SH intensity scales quadratically with the number of molecules in the focal volume (*42*). Even at the highest polyelectrolyte concentration used here, there are still >1000 water molecules per monomer, leading to a theoretical 10^6 higher contribution from the water than from the polyelectrolytes.

Figure 1D also shows that a significant discrepancy occurs when the same fs-ESHS experiment is conducted using D_2O as the solvent instead of H_2O. The fs-ESHS trend for D_2O is significantly altered compared to H_2O: The maximum intensity is 2.4× lower and appears at a 1.5× higher concentration (ionic strength) compared to H_2O. The presence of a saturation intensity at high concentration, a low-onset ionic strength, and the difference between H_2O and D_2O are reminiscent of the observations for aqueous salt solutions of Fig. 1A. The main difference here is the appearance of a pronounced peak in the concentration curve compared to electrolyte solutions. This behavior stems from the interactions between the electrostatic field of the ionic groups on polyelectrolytes and the H-bond network of water. At very low ionic strength, the polyelectrolyte chains are in an extended conformation due to strong intrachain electrostatic repulsion (*43*–*46*) and different polyelectrolytes are expected to be correlated with each other (*38*, *47*–*49*). The ionized groups on the polyelectrolyte chains therefore do not move freely like simple electrolyte ions but are limited in their spatial arrangement by both the limited flexibility of the polyelectrolyte chains and the interactions between different chains. These intra- and interchain correlations affect the orientational order of water molecules that are associated with each ionic group as extended hydration shells. The long-range correlations in polyelectrolyte solutions arise from a combination of a high degree of ionization of the polyelectrolytes and a large Debye screening length. At an ionic strength of $I = 10\ \mu M$, the Debye length is $\kappa^{-1} = (2\pi\lambda_B/10^3 N_A I)^{1/2} \approx 100$ nm, where λ_B is the Bjerrum length as defined before and N_A is the Avogadro number. Because the ionic strength is a function of polyelectrolyte concentration, increasing the polyelectrolyte concentration shortens the Debye length, which suppresses long-range spatial correlations (*43*, *44*, *49*). The importance of Debye screening for the fs-ESHS response was confirmed by measuring the effect of varying ionic strength on the measured fs-ESHS intensity shown in fig. S2. The fs-ESHS intensity drops rapidly with ionic strength and virtually disappears above 1 mM. The total electrostatic field in the liquid, and consequently the water-water correlations that are induced by it, is expected to be the highest when the chain concentration is maximized up to the point where the spatial correlations between the polyelectrolyte chains begin to disappear due to Debye screening. Such a behavior would give rise to a maximum in the fs-ESHS response. For PAA in H_2O, the fs-ESHS intensity maximum occurs at an ionic strength of ~24 μM, which corresponds to a Debye length of 62 nm.

Viscosity

The fs-ESHS data of Fig. 1D suggest an unusually large degree of polyelectrolyte-induced orientational correlations between the water molecules. Would such an increase in correlations also have an influence on a macroscopic observable? Viscosity is a good candidate, because the degree of structural correlations in a solvent has a significant influence on viscosity (*25*, *50*–*53*). This is apparent in the 23% higher viscosity of pure D_2O compared to H_2O at room temperature (*54*, *55*), which cannot be entirely accounted for by a difference in mass (moment of inertia) of the two isotopes of water. The residual difference in viscosity is due to stronger H-bonding in D_2O (*53*, *56*). Recent work from our group has shown that there is an ion-specific correlation between the viscosity and the intensity of fs-ESHS experiments for high electrolyte concentrations (*57*). Studies from as early as the 1950s have reported an anomalous increase in the reduced specific viscosity of dilute aqueous polyelectrolyte solutions, which does not occur for neutral polymers or at high ionic strength (*47*, *58*). The viscosity anomaly was qualitatively explained in terms of intra- and inter-polyelectrolyte correlations (*38*, *39*, *59*). In light of the recent fs-ESHS experiments, it would be interesting to investigate whether long-range electrostatic interactions between the charges and the H-bond network in polyelectrolyte aqueous solutions play a role in this viscosity anomaly. Traditional viscosity models are based on a mean-field approximation of the solvent and therefore do not explicitly take into account changes in solvent structure. Experimentally performing specific viscosity and fs-ESHS measurements will show whether a long-range interaction between the electrostatic field and the H-bond network of water is playing a role in the viscous flow of polyelectrolyte solutions.

In what follows, we investigate the long-range correlations in aqueous polyelectrolyte solutions in more detail by measuring the integrated SH intensity scattered in the forward half-plane (Fig. 2A) and compare it with the reduced specific viscosity of the solutions (Fig. 2B). In Fig. 2A, the measured integrated fs-ESHS intensity (S_{int}) is plotted as a function of polyelectrolyte concentration (bottom axis) and ionic strength (top axis) for PAA solutions in H_2O (red circles) and D_2O (blue squares) and for poly(ethylene glycol) (PEG), a neutral polymer dissolved in H_2O (green triangles). The fs-ESHS data for PSS are shown in fig. S3 and display a similar trend as the PAA. The concentration dependence of S_{int} is comparable to the fixed-angle measurements of Fig. 1D, but higher fs-ESHS intensities are recorded, allowing a more accurate comparison. The fs-ESHS intensity increases up to a value of 80 times the scattered intensity of pure water up to a concentration of ~9 nM (ionic strength of ~10 μM). The intensity drops with further addition of PAA, leveling off at a concentration of 220 nM (ionic strength of 240 μM). For D_2O solutions, the behavior is also similar compared to Fig. 1D and shows a curve that is reduced in maximum intensity by a factor of ~4 and shifted to eight times higher concentrations. The results for PSS (fig. S3) are qualitatively similar but display an even more pronounced difference between H_2O and D_2O: The fs-ESHS peak intensity is reduced from 80 to 8, and the peak polymer concentration is increased by a factor of 14. PEG, on the other hand, shows no such behavior, underlining the importance of the electrostatic interactions with water.

The measured reduced specific viscosity, η_{red}, as a function of polymer concentration is shown for PAA solutions in H_2O (red) and D_2O (blue) in Fig. 2B. The reduced specific viscosity is calculated by $\eta_{red} = (\eta_{solution} - \eta_{water})/c_m\eta_{solution}$, where η_i is the measured dynamic viscosity and c_m is the monomer concentration. The data for the PSS polyelectrolyte are plotted in the same manner and are shown in fig. S3. As a comparison, the specific viscosity of neutral PEG polymer chains in H_2O is also displayed (green trace). The η_{red} of PEG was theoretically calculated with details shown in section S4. The specific viscosity of

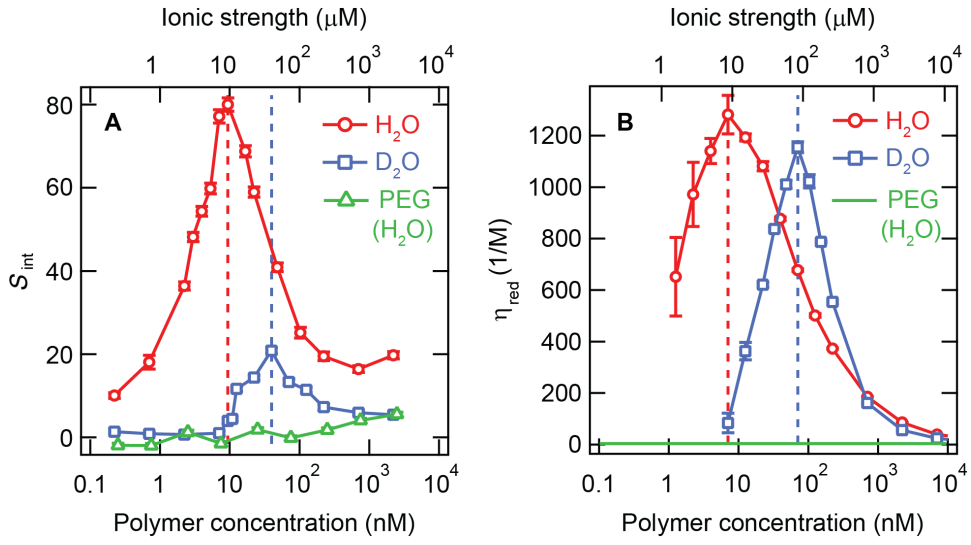

Fig. 2. Polyelectrolytes induce strong orientational correlations leading to viscosity changes. (**A**) fs-ESHS intensities, relative to that of pure H_2O/D_2O, of PAA obtained by integrating the fs-ESHS intensity in the angular range $-90° > \theta > 90°$. The dashed line indicates the peak concentration. The data for PEG in H_2O (green) serve as a comparison with a neutral polymer. The data were recorded, with all beams polarized parallel to the horizontal scattering plane (PPP). (**B**) Reduced specific viscosity of PAA dissolved in H_2O and D_2O. The average molecular weight of PAA was 450 kDa, corresponding to a contour length of 1560 nm. The reduced specific viscosity of PEG was calculated using the Huggins equation (*74*), with details of the calculations shown in section S4.

PAA and PSS shows a surprisingly similar behavior as the fs-ESHS data, starting at a low value and then going over a maximum with increasing concentration. The maximum occurs at the same ionic strength as the fs-ESHS maximum (~10 μM for H_2O) and comprises a difference of two orders of magnitude in the η_{red}. The effect of D_2O on the viscosity is similar: The peak intensity is shifted to higher ionic strength for D_2O (~ 100 μM), and the peak value is reduced by ~20%. For PSS (fig. S3), the effect is even more pronounced: Switching from H_2O to D_2O, the peak concentrations are shifted from 3.2 to 100 nM (ionic strength of 2.8 to 85 μM), and the peak value of η_{red} is reduced by a factor of ~3.

The appearance of a peak in η_{red} as a function of polyelectrolyte concentration is in qualitative agreement with previously measured data for both PAA (*60*) and PSS (*38*, *61*) in H_2O. To the best of our knowledge, the D_2O measurements have not been reported before and are remarkably different from H_2O in that the peak occurs at 10× higher concentration and with a smaller amplitude. The anomalous viscosity peak is known to rapidly disappear when excess salt is added to the solution due to Debye screening (*62*), which is consistent with the sensitivity of the fs-ESHS response to added salt shown in fig. S2. This points to long-range electrostatics as the source for the observed behavior in both the molecular structural (fs-ESHS) measurement and the macroscopic (reduced viscosity) measurement. The neutral PEG (and other neutral polymers) does not display the viscosity anomaly (*63*, *64*). Likewise, there is no peak in the fs-ESHS response of PEG. This further confirms the importance of long-range electrostatic interactions in PAA (PSS) solutions, which are responsible for the strong enhancement of the fs-ESHS response and the reduced viscosity and are absent for neutral polymers such as PEG.

The behavior observed in Fig. 2 is interesting for the following reasons: First, the correlation between the fs-ESHS intensity and the reduced specific viscosity for both H_2O and D_2O and for both polyelectrolytes with different molecular weights and different chemical structures suggests that they derive (at least partially) from the same mechanism. Second, the isotope effect observed in the viscosity is unexpected. According to literature, the anomalous behavior of the specific viscosity of polyelectrolyte solutions stems solely from intra- and inter-polyelectrolyte correlations (*38*, *39*, *48*). These models are in agreement with the experimental data in H_2O. However, because they are based on a mean-field approximation of water, they do not predict a significant difference in the reduced specific viscosity between H_2O and D_2O, as the dielectric constants of the two solvents differ by less than 0.4% (*65*). Using one of the existing mean-field models (*66*), we calculated the reduced specific viscosity and plotted it together with the measured data for H_2O and D_2O. The data are presented in fig. S4. Although the model reproduces the anomaly for PAA in H_2O, it predicts nearly the same behavior for D_2O. Yet, the measured η_{red} of PAA is significantly different for D_2O, indicating that the enhancement of water-water correlations plays an important role.

As mentioned in the Introduction, the fs-ESHS data for simple electrolyte solutions in Fig. 1A are different for H_2O and D_2O. This difference was attributed to nuclear quantum effects. H-bonds between water molecules can be broken along two different orthogonal axes. Figure 1B illustrates two H-bonded water molecules that are orientationally correlated, and the black arrows illustrate the two axes of motion: a stretching motion or a rotational motion. The stretching motion does not lead to differences in orientational correlations in contrast to the rotations, rendering fs-ESHS more sensitive to H-bond breaking via rotation. Because the H-bond bending mode is predicted to be stronger in D_2O than in H_2O (*22*, *67*, *68*), the fs-ESHS response of pure D_2O is larger than that of H_2O (*24*), as is its resistance to restructuring due to ions (*24*) or ionic groups on polyelectrolytes as is observed here. Because the fs-ESHS data and the specific viscosity data are similar, it is plausible that a similar decoupling effect also contributes to viscosity. Viscosity depends on the movement of molecules through water, and this

naturally involves the breaking of H-bonds (*69*). Our combined data suggest that the breaking of H-bonds by rotation plays a relatively larger role in determining the viscosity than the breaking of H-bonds by stretching. Namely, if both modes would contribute equally, no viscosity difference between H_2O and D_2O solutions would be observed. If the stretching mode would contribute more, then the D_2O/H_2O difference would be reversed. Our observation and assessment are in agreement with spectroscopic measurements, because the H-bond stretch mode was detected at ~183 cm^{-1}, while the H-bond bending mode was found to occur at lower frequencies of ~50 cm^{-1} (for H_2O) (*70*, *71*). Although both values are below the thermal energy (219 cm^{-1} at room temperature), the bending mode is energetically more favorable and therefore may contribute more than the stretching mode. Such a mechanism could also explain an isotope effect observed in adhesion hysteresis (*72*). Thus, long-range interactions are present in more systems than simple electrolyte solutions and can lead to marked changes in macroscopic properties as well as unexpected significant nuclear quantum effects. As water plays an omnipresent role in diverse disciplines as physics, chemistry, biology, and medicine, the observed effects can have consequences for processes where charges are involved.

SUMMARY AND CONCLUSIONS

We investigated long-range interactions between polyelectrolytes and the H-bond network of water. We found an increase in the orientational order of water and an even larger difference between H_2O and D_2O solutions compared to simple electrolyte solutions. Upon increasing the polyelectrolyte concentration, the fs-ESHS intensity increases up to a maximum and then reduces and levels off. Qualitatively, this behavior can be explained by two parallel effects: increasing polyelectrolyte number density and screening of the electrostatic field by counterions. Macroscopically, we observed a similar behavior for the reduced viscosity. The reduced viscosity changes up to two orders of magnitude with increasing concentration, shifts by a factor of ~8 to 14 in the concentration, and decreases in maximum value (20 to 300%) when D_2O is used instead of H_2O. Traditional mean-field models cannot explain such a difference. We conclude that the anomalous viscosity of polyelectrolyte solutions cannot be entirely explained by intra- and inter-polyelectrolyte correlations but that changes in water-water orientational correlations also influence the reduced viscosity. Moreover, our data suggest that H-bond breaking through rotations occurs more readily than through H-bond stretching and is more important for viscous flow.

MATERIALS AND METHODS

Chemicals and sample preparation

PAA (molecular weight of 450 kDa; Polysciences Inc.), sodium PSS, sodium salt (molecular weight of 1000 kDa; Polysciences Inc.), and PEG (molecular weight of 400 kDa; Sigma) in powder were used as received. NaCl (99.999%) was purchased from Acros. Stock polymer solutions were prepared by dissolving the powder in water (H_2O or D_2O). The samples were prepared by subsequent dilution of the stock solutions to obtain the desired polymer concentration. Stock NaCl solutions were filtered through Millipore Millex-VV 0.1-mm polyvinylidene difluoride membrane filters. Ultrapure H_2O with an electrical resistance of 18.2 MΩ·cm was obtained from a Milli-Q UF-Plus instrument (Millipore Inc.). For experiments with heavy water, the D_2O used was 99.8% D atoms with an electrical resistance of >2 MΩ·cm (Armar).

fs-ESHS setup and measurements

Laser pulses (190 fs) centered at 1028 nm with a 200-kHz repetition rate were used as the light source for fs-ESHS measurements. The polarization of the input pulses was controlled by a Glan-Taylor polarizer (GT10-B, Thorlabs) and a zero-order half–wave plate (WPH05M-1030). The incident laser pulses, filtered by a long pass filter (FEL0750, Thorlabs), with a pulse energy of 0.3 μJ (incident laser power P = 60 mW), were focused into a cylindrical glass cuvette cell (inner diameter of 4.2 mm; LS Instruments) with a waist diameter of 35 μm and a Rayleigh length of 0.94 mm. Scattered SH light was collected with a plano-convex lens (f = 5 cm) and then filtered with a 10- or 50-nm bandpass filter centered around 515 nm (ET515/10 and ET515/50, Chroma). A Glan-Taylor polarizer (GT10-A, Thorlabs) was used for the polarization analysis of the SH light. Last, the SH light was focused into a gated photomultiplier tube (H7421-40, Hamamatsu). More details on the setup can be found in (*73*).

The experimental conditions used for fixed-angle measurements were the same as in (*24*, *30*, *57*). The detection angle was set to 90° with an acceptance angle of 11.4°. Each data point is an average of three to five measurements. Each measurement is an average of 50 expositions of 1-s integration time, using $50 \times 2 \times 10^5$ pulses in total. The gate width was 10 ns.

To compare fs-ESHS response with reduced specific viscosity, we introduced a different metric: integrated fs-ESHS intensity (S_{int}). To obtain this quantity, a scattering pattern is recorded at 5° steps between −90° and +90° with an opening angle of 3.4°. The pattern is normalized at each angle θ with respect to pure water: $S(\theta) = (I_{PPP,solution}(\theta) - I_{PPP,water}(\theta))/I_{SSS,water}(\theta)$, where $I(\theta)$ stands for the average SH count rate at a scattering angle θ and the subscripts PPP and SSS stand for polarization combinations (P = parallel and S = perpendicular with respect to the horizontal scattering plane), denoted in this order: second harmonic, fundamental, fundamental. The integrated normalized fs-ESHS intensity is calculated as $S_{int} = \Sigma S(\theta)$ for all $\theta \neq 0°$.

Dynamic viscosity measurements

Viscosities were measured using an Ubbelohde-type glass capillary viscometer (Paragon Scientific Ltd.) immersed in a temperature-controlled water bath (ET 15S, Lauda Scientific GmbH). The measurements were performed at 25.00° ± 0.01°C. The viscometer with the liquid was allowed to reach equilibrium with the bath for at least 4 min before a measurement. The elution times were measured with a time-stamped digital camera (720 pixels at 24 frames per second, Huawei Mi A1) that recorded the passing of the liquid's meniscus between the two marked positions on the viscometer. Each sample was measured at least three times.

SUPPLEMENTARY MATERIALS

Supplementary material for this article is available at http://advances.sciencemag.org/cgi/content/full/5/12/eaay1443/DC1

Section S1. Hyper-Rayleigh scattering from polyelectrolytes
Section S2. Dependence of fs-ESHS from PAA on excess salt concentration
Section S3. fs-ESHS and reduced viscosity of PSS
Section S4. Calculation of the reduced specific viscosity of PEG
Section S5. Modeling the reduced specific viscosity of PAA
Fig. S1. Negligible contribution of polyelectrolytes to SH scattering.
Fig. S2. fs-ESHS response disappears with addition of salt.
Fig. S3. Polyelectrolytes induce strong orientational correlations leading to viscosity changes.
Fig. S4. Reduced specific viscosity calculation.

REFERENCES AND NOTES

1. E. Leontidis, Hofmeister anion effects on surfactant self-assembly and the formation of mesoporous solids. *Curr. Opin. Colloid Interface Sci.* **7**, 81–91 (2002).
2. S. K. Pal, L. Zhao, A. H. Zewail, Water at DNA surfaces: Ultrafast dynamics in minor groove recognition. *Proc. Natl. Acad. Sci. U.S.A.* **100**, 8113–8118 (2003).
3. B. Jayaram, T. Jain, The role of water in protein-DNA recognition. *Annu. Rev. Biophys. Biomol. Struct.* **33**, 343–361 (2004).
4. S. McLaughlin, G. Szabo, G. Eisenman, Divalent ions and the surface potential of charged phospholipid membranes. *J. Gen. Physiol.* **58**, 667–687 (1971).
5. U. Raviv, S. Giasson, N. Kampf, J. F. Gohy, R. Jérôme, J. Klein, Lubrication by charged polymers. *Nature* **425**, 163–165 (2003).
6. H. D. B. Jenkins, Y. Marcus, Viscosity B-coefficients of ions in solution. *Chem. Rev.* **95**, 2695–2724 (1995).
7. Y. Marcus, Effect of ions on the structure of water: Structure making and breaking. *Chem. Rev.* **109**, 1346–1370 (2009).
8. W. Kunz, *Specific Ion Effects* (World Scientific, 2010).
9. I. Waluyo, D. Nordlund, U. Bergmann, D. Schlesinger, L. G. M. Pettersson, A. Nilsson, A different view of structure-making and structure-breaking in alkali halide aqueous solutions through x-ray absorption spectroscopy. *J. Chem. Phys.* **140**, 244506 (2014).
10. A. K. Soper, K. Weckström, Ion solvation and water structure in potassium halide aqueous solutions. *Biophys. Chem.* **124**, 180–191 (2006).
11. A. W. Omta, M. F. Kropman, S. Woutersen, H. J. Bakker, Negligible effect of ions on the hydrogen-bond structure in liquid water. *Science* **301**, 347–349 (2003).
12. Q. Sun, Raman spectroscopic study of the effects of dissolved NaCl on water structure. *Vib. Spectrosc.* **62**, 110–114 (2012).
13. R. Li, Z. Jiang, F. Chen, H. Yang, Y. Guan, Hydrogen bonded structure of water and aqueous solutions of sodium halides: A Raman spectroscopic study. *J. Mol. Sci.* **707**, 83–88 (2004).
14. M. Kondoh, Y. Ohshima, M. Tsubouchi, Ion effects on the structure of water studied by terahertz time-domain spectroscopy. *Chem. Phys. Lett.* **591**, 317–322 (2014).
15. A. P. Gaiduk, G. Galli, Local and global effects of dissolved sodium chloride on the structure of water. *J. Phys. Chem. Lett.* **8**, 1496–1502 (2017).
16. B. Hribar, N. T. Southall, V. Vlachy, K. A. Dill, How ions affect the structure of water. *J. Am. Chem. Soc.* **124**, 12302–12311 (2002).
17. J. D. Smith, R. J. Saykally, P. L. Geissler, The effects of dissolved halide anions on hydrogen bonding in liquid water. *J. Am. Chem. Soc.* **129**, 13847–13856 (2007).
18. E. Pluharova, P. Jungwirth, N. Matubayasi, O. Marsalek, Structure and dynamics of the hydration shell: Spatially decomposed time correlation approach. *J. Chem. Theory Comput.* **15**, 803–812 (2018).
19. W. Kunz, Specific ion effects in liquids, in biological systems, and at interfaces. *Pure Appl. Chem.* **78**, 1611–1617 (2006).
20. Y. Zhang, P. S. Cremer, Chemistry of Hofmeister anions and osmolytes. *Annu. Rev. Phys. Chem.* **61**, 63–83 (2010).
21. H. I. Okur, J. Hladílková, K. B. Rembert, Y. Cho, J. Heyda, J. Dzubiella, P. S. Cremer, P. Jungwirth, Beyond the Hofmeister series: Ion-specific effects on proteins and their biological functions. *J. Phys. Chem. B* **121**, 1997–2014 (2017).
22. X.-Z. Li, B. Walker, A. Michaelides, Quantum nature of the hydrogen bond. *Proc. Natl. Acad. Sci. U.S.A.* **108**, 6369–6373 (2011).
23. U. Bergmann, D. Nordlund, P. Wernet, M. Odelius, L. G. M. Pettersson, A. Nilsson, Isotope effects in liquid water probed by x-ray Raman spectroscopy. *Phys. Rev. B* **76**, 024202 (2007).
24. Y. Chen, H. I. Okur, N. Gomopoulos, C. Macias-Romero, P. S. Cremer, P. B. Petersen, D. M. Wilkins, C. Liang, M. Ceriotti, S. Roke, Electrolytes induce long-range orientational order and free energy changes in the H-bond network of bulk water. *Sci. Adv.* **2**, e1501891 (2016).
25. S. Perticaroli, B. Mostofian, G. Ehlers, J. C. Neuefeind, S. O. Diallo, C. B. Stanley, L. Daemen, T. Egami, J. Katsaras, X. Cheng, J. D. Nickels, Structural relaxation, viscosity, and network connectivity in a hydrogen bonding liquid. *Phys. Chem. Chem. Phys.* **19**, 25859–25869 (2017).
26. D. M. Wilkins, D. E. Manolopoulos, S. Roke, M. Ceriotti, Communication: Mean-field theory of water-water correlations in electrolyte solutions. *J. Chem. Phys.* **146**, 181103 (2017).
27. J. Duboisset, P.-F. Brevet, Salt-induced long-to-short range orientational transition in water. *Phys. Rev. Lett.* **120**, 263001 (2018).
28. L. Belloni, D. Borgis, M. Levesque, Screened coulombic orientational correlations in dilute aqueous electrolytes. *J. Phys. Chem. Lett.* **9**, 1985–1989 (2018).
29. D. Borgis, L. Belloni, M. Levesque, What does second harmonic scattering measure in diluted electrolytes? *J. Phys. Chem. Lett.* , (2018).
30. Y. Chen, N. Dupertuis, H. I. Okur, S. Roke, Temperature dependence of water-water and ion-water correlations in bulk water and electrolyte solutions probed by femtosecond elastic second harmonic scattering. *J. Chem. Phys.* **148**, 222835 (2018).
31. R. Bersohn, Y. H. Pao, H. Frisch, Double-quantum light scattering by molecules. *J. Chem. Phys.* **45**, 3184–3198 (1966).
32. S. Ong, X. Zhao, K. B. Eisenthal, Polarization of water molecules at a charged interface: Second harmonic studies of the silica/water interface. *Chem. Phys. Lett.* **191**, 327–335 (1992).
33. G. Tocci, C. Liang, D. M. Wilkins, S. Roke, M. Ceriotti, Second-harmonic scattering as a probe of structural correlations in liquids. *J. Phys. Chem. Lett.* **7**, 4311–4316 (2016).
34. K. Clays, A. Persoons, Hyper-Rayleigh scattering in solution. *Phys. Rev. Lett.* **66**, 2980–2983 (1991).
35. H. I. Okur, Y. Chen, D. M. Wilkins, S. Roke, The Jones-Ray effect reinterpreted: Surface tension minima of low ionic strength electrolyte solutions are caused by electric field induced water-water correlations. *Chem. Phys. Lett.* **684**, 433–442 (2017).
36. H. I. Okur, C. I. Drexler, E. C. Tyrode, P. S. Cremer, S. Roke, The Jones-Ray effect is not caused by surface active impurities. *J. Phys. Chem. Lett.* , (2018).
37. P. Jungwirth, D. Laage, Ion-induced long-range orientational correlations in water: Strong or weak, physiologically relevant or unimportant, and unique to water or not? *J. Phys. Chem. Lett.* **9**, 2056–2057 (2018).
38. J. Cohen, Z. Priel, Y. Rabin, Viscosity of dilute polyelectrolyte solutions. *J. Chem. Phys.* **88**, 7111–7116 (1988).
39. K. Nishida, K. Kaji, T. Kanaya, Theoretical calculation of reduced viscosity of polyelectrolyte solutions. *Polymer* **42**, 8657–8662 (2001).
40. G. S. Manning, Limiting laws and counterion condensation in polyelectrolyte solutions I. colligative properties. *J. Chem. Phys.* **51**, 924–933 (1969).
41. G. S. Manning, The critical onset of counterion condensation: A survey of its experimental and theoretical basis. *Ber. Bunsen. Phys. Chem.* **100**, 909–922 (1996).
42. R. W. Boyd, *Nonlinear Optics* (Elsevier, 2008).
43. T. Odijk, Polyelectrolytes near the rod limit. *J. Polym. Sci.* **15**, 477–483 (1977).
44. J. Skolnick, M. Fixman, Electrostatic persistence length of a wormlike polyelectrolyte. *Macromolecules* **10**, 944–948 (1977).
45. S. Lifson, A. Katchalsky, The electrostatic free energy of polyelectrolyte solutions. II. Fully stretched macromolecules. *J. Polym. Sci.* **13**, 43–55 (1954).
46. M. J. Stevens, K. Kremer, The nature of flexible linear polyelectrolytes in salt free solution: A molecular dynamics study. *J. Chem. Phys.* **103**, 1669–1690 (1995).
47. H. Eisenberg, J. Pouyet, Viscosities of dilute aqueous solutions of a partially quaternized poly-4-vinylpyridine at low gradients of flow. *J. Polym. Sci.* **13**, 85–91 (1954).
48. M. Antonietti, A. Briel, S. Förster, Intrinsic viscosity of small spherical polyelectrolytes: Proof for the intermolecular origin of the polyelectrolyte effect. *J. Chem. Phys.* **105**, 7795–7807 (1996).
49. K. Nishida, K. Kaji, T. Kanaya, T. Shibano, Added salt effect on the intermolecular correlation in flexible polyelectrolyte solutions: Small-angle scattering study. *Macromolecules* **35**, 4084–4089 (2002).
50. R. Fort, W. Moore, Viscosities of binary liquid mixtures. *Trans. Faraday Soc.* **62**, 1112–1119 (1966).
51. W. J. Lamb, J. Jonas, NMR study of compressed supercritical water. *J. Chem. Phys.* **74**, 913–921 (1981).
52. C. Cho, J. Urquidi, G. W. Robinson, Molecular-level description of temperature and pressure effects on the viscosity of water. *J. Chem. Phys.* **111**, 10171–10176 (1999).
53. M. Ceriotti, W. Fang, P. G. Kusalik, R. H. McKenzie, A. Michaelides, M. A. Morales, T. E. Markland, Nuclear quantum effects in water and aqueous systems: Experiment, theory, and current challenges. *Chem. Rev.* **116**, 7529–7550 (2016).
54. F. J. Millero, R. Dexter, E. Hoff, Density and viscosity of deuterium oxide solutions from 5-70. deg. *J. Chem. Eng. Data* **16**, 85–87 (1971).
55. L. Korson, W. Drost-Hansen, F. J. Millero, Viscosity of water at various temperatures. *J. Phys. Chem.* **73**, 34–39 (1969).
56. A. Berger, G. Ciardi, D. Sidler, P. Hamm, A. Shalit, Impact of nuclear quantum effects on the structural inhomogeneity of liquid water. *Proc. Natl. Acad. Sci. U.S.A.* **116**, 2458–2463 (2019).
57. Y. Chen, H. I. Okur, C. Liang, S. Roke, Orientational ordering of water in extended hydration shells of cations is ion-specific and is correlated directly with viscosity and hydration free energy. *Phys. Chem. Chem. Phys.* **19**, 24678–24688 (2017).
58. D. T. F. Pals, J. J. Hermans, Sodium salts of pectin and of carboxy methyl cellulose in aqueous sodium chloride. I. Viscosities. *Rec. Trav. Chim. Pays-Bas* **71**, 433–457 (1952).
59. M. Shibayama, R. Moriwaki, F. Ikkai, S. Nomura, Viscosity behaviour of weakly charged polymer-ion complexes comprising poly(vinyl alcohol) and Congo red. *Polymer* **35**, 5716–5721 (1994).
60. A. Fernandes, R. Martins, C. da Trindade Neto, M. Pereira, J. Fonseca, Characterization of polyelectrolyte effect in poly (acrylic acid) solutions. *J. Appl. Polym. Sci.* **89**, 191–196 (2003).
61. I. Roure, M. Rinaudo, M. Milas, E. Frollini, Viscometric behaviour of polyelectrolytes in the presence of low salt concentration. *Polymer* **39**, 5441–5445 (1998).
62. J. Cohen, Z. Priel, Viscosity of dilute polyelectrolyte solutions: Concentration dependence on sodium chloride, magnesium sulfate and lanthanum nitrate. *Macromolecules* **22**, 2356–2358 (1989).

63. D. Thomas, A. Charlesby, Viscosity relationship in solutions of polyethylene glycols. *J. Polym. Sci.* **42**, 195–202 (1960).
64. I. Shulyak, E. Grushova, A. Semenchenko, Rheological properties of aqueous solutions of polyethylene glycols with various molecular weights. *Russ. J. Phys. Chem.* **85**, 419–422 (2011).
65. J. Wyman Jr., E. Ingalls, The dielectric constant of deuterium oxide. *J. Am. Chem. Soc.* **60**, 1182–1184 (1938).
66. S. A. Rice, J. G. Kirkwood, On an approximate theory of transport in dense media. *J. Chem. Phys.* **31**, 901–908 (1959).
67. S. Habershon, T. E. Markland, D. E. Manolopoulos, Competing quantum effects in the dynamics of a flexible water model. *J. Chem. Phys.* **131**, 024501 (2009).
68. P. V. Escribá, J. M. González-Ros, F. M. Goñi, P. K. J. Kinnunen, L. Vigh, L. Sánchez-Magraner, A. M. Fernández, X. Busquets, I. Horváth, G. Barceló-Coblijn, Membranes: A meeting point for lipids, proteins and therapies. *J. Cell. Mol. Med.* **12**, 829–875 (2008).
69. D. Laage, J. T. Hynes, A molecular jump mechanism of water reorientation. *Science* **311**, 832–835 (2006).
70. J. K. Vij, D. R. J. Simpson, O. E. Panarina, Far infrared spectroscopy of water at different temperatures: GHz to THz dielectric spectroscopy of water. *J. Mol. Liq.* **112**, 125–135 (2004).
71. J.-B. Brubach, A. Mermet, A. Filabozzi, A. Gerschel, P. Roy, Signatures of the hydrogen bonding in the infrared bands of water. *J. Chem. Phys.* **122**, 184509 (2005).
72. G. Y. Choi, A. Ulman, Y. Shnidman, W. Zurawsky, C. Fleischer, Isotope effect in adhesion. *J. Phys. Chem. B* **104**, 5768–5771 (2000).
73. N. Gomopoulos, C. Lütgebaucks, Q. Sun, C. Macias-Romero, S. Roke, Label-free second harmonic and hyper Rayleigh scattering with high efficiency. *Opt. Express* **21**, 815–821 (2013).
74. M. L. Huggins, The viscosity of dilute solutions of long-chain molecules. IV. Dependence on concentration. *J. Am. Chem. Soc.* **64**, 2716–2718 (1942).

Acknowledgments

Funding: This work was supported by the Julia Jacobi Foundation, the European Research Council (grant number 616305), and the EPFL-WIS Fund. **Author contributions:** J.D. and H.I.O. performed experimental measurements. J.D. performed analytical computations and modeling. S.R. and J.D. wrote the manuscript. S.R. conceived and supervised the work and contributed to the data interpretation. **Competing interests:** The authors declare that they have no competing interests. **Data and materials availability:** All data needed to evaluate the conclusions in the paper are present in the paper and/or the Supplementary Materials. Additional data related to this paper may be requested from the authors.

Submitted 24 May 2019
Accepted 22 October 2019
Published 6 December 2019
10.1126/sciadv.aay1443

Citation: J. Dedic, H. I. Okur, S. Roke, Polyelectrolytes induce water-water correlations that result in dramatic viscosity changes and nuclear quantum effects. *Sci. Adv.* **5**, eaay1443 (2019).

Polyelectrolytes induce water-water correlations that result in dramatic viscosity changes and nuclear quantum effects

J. Dedic, H. I. Okur and S. Roke

Sci Adv **5** (12), eaay1443.
DOI: 10.1126/sciadv.aay1443